

Helical Transition-Metal Complexes of Constrained 2,2'-Bidipyrriins

Martin Bröring,^{*,[a]} Stephan Link,^[a] Carsten D. Brandt,^[a] and Esther Cónsul Tejero^[a]

Keywords: 2,2'-Bidipyrriins / Helicates / Constrained ligands / Porphyrinoids / Coordination modes

Nickel(II), palladium(II), zinc(II) and copper(II) complexes of new constrained 2,2'-bidipyrriin ligands (H₂BDP) with a peripheral eight-membered ring were prepared and examined with respect to coordination modes and conformation. Ni^{II} and Pd^{II} ions form mononuclear complexes with a distorted square-planar N₄ coordination, which was determined for the palladium derivative by single-crystal X-ray diffraction.

Zn^{II} ions lead to the formation of dinuclear M₂L₂ helicates, and for Cu^{II} ions both coordination modes are realized. X-ray crystallographic analyses reveal short M...M distances for the dinuclear helicates of Cu^{II} and Zn^{II} bidipyrriins and individually distinct packing patterns for both in the solid state. (© Wiley-VCH Verlag GmbH & Co. KGaA, 69451 Weinheim, Germany, 2007)

Introduction

For a long time the coordination chemistry of open-chain tetrapyrroles was limited to bioinspired studies on the metal-binding capabilities of biliverdin-IX α (BV) and closely related model ligands.^[1] Naturally occurring heme degradation processes^[2] and the unexpected lability of Fe–BV complexes^[3] have been the major driving forces for this research, and many questions have remained unanswered until today. Open-chain tetrapyrroles with a non-natural backbone, on the other hand, have been prepared mainly as precursors for different template-directed macrocyclizations to porphyrinoids.^[4] Signs of a stand-alone coordination chemistry of such ligands hardly appeared in the literature prior to 1990.^[5]

The interest in open-chain tetrapyrroles as multifunctional chelate ligands started in 1996 with Mizutani's work on the chiral recognition of amino acids by helical Zn–BV derivatives.^[6] In 1998 two groups reported, independently, that open-chain oligopyrroles are useful templates for the construction of supramolecular coordination assemblies,^[7] including earlier findings on similar dinuclear species.^[8] A very elegant approach along this line was reported by Thompson et al., who introduced chiral carboxylic ester side chains in order to investigate stereoselective helix formation triggered by metal insertion.^[9] The first bioinorganic use of linear tetrapyrroles besides heme degradation studies was reported in 2001.^[10] It could be demonstrated that a dimeric manganese(III) complex of BV-IX α -dimethyl ester catalyzes the decomposition of hyperoxide, and that therefore this complex should be addressed as a functional SOD model. However, reports on investigations of possible medical applications have not yet appeared.

A tetrapyrrolic system with a particularly simple architecture is found in the non-natural 2,2'-bidipyrriin,^[7b,11] which is constituted of two directly linked dipyrriin units, and which can in principle rotate around this central pyrrole–pyrrole link. 2,2'-Bidipyrriins have been shown in recent years to support a multitude of different coordination modes (Figure 1).^[12] Because of the robustness of methyl-terminated 2,2'-bidipyrriins and their straightforward preparation in large amounts, these ligands would be an ideal candidate for a reference system of the natural BV-IX α and especially of the hitherto almost elusive iron complexes thereof.^[13] Unfortunately, however, and similar to other natural and non-natural open-chain tetrapyrroles, 2,2'-bidipyrriins do not form sufficiently stable iron chelates.

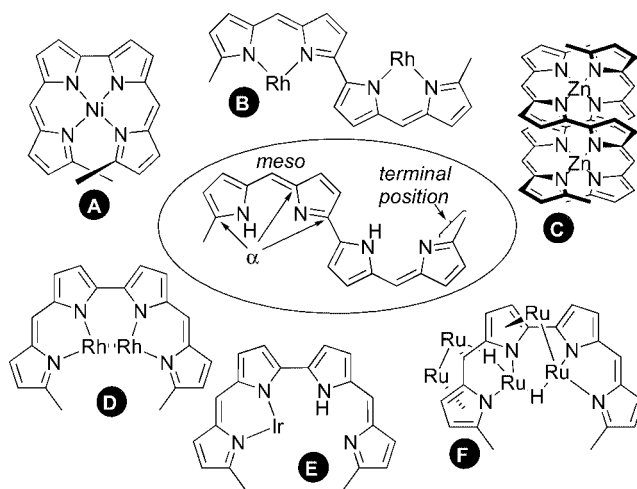


Figure 1. Nomenclature and selected coordination compounds with different binding modes (A–F) of 2,2'-bidipyrriins (alkyl substituents and CO coligands on Rh, Ir and Ru omitted).

[a] Fachbereich Chemie, Philipps-Universität Marburg, Hans-Meerwein-Straße, 35032 Marburg, Germany
Fax: +49-6421-282-5653
E-mail: Martin.Broering@chemie.uni-marburg.de

2,2'-Bidipyrins typically reside in an *anti* conformation in the solid state and in solution,^[11b,11c,14] and we expected that, enforcing a *syn*- (or *syn-gauche*-) conformation as shown on the right in Figure 2, the formation of 1:1 chelate complexes of type **A** with kinetically labile ions should be favoured. We report here on the synthesis of such conformationally restricted 2,2'-bidipyrins **1** and **2** and their coordination behaviour to 3d transition metals.

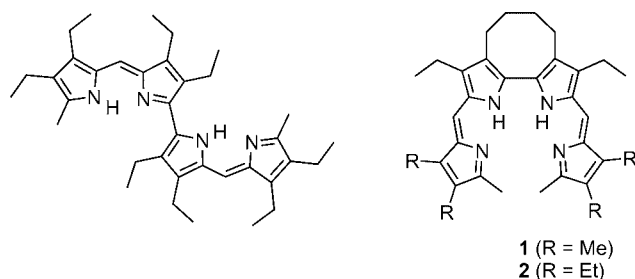
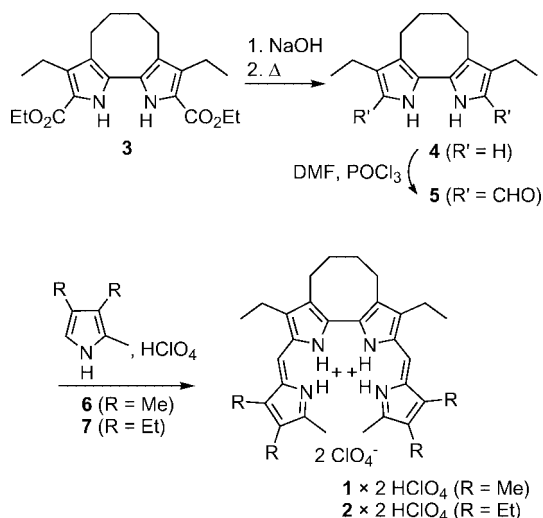


Figure 2. Conformational preferences of unrestrained and restrained 2,2'-bidipyrins.

Results and Discussion

The synthesis of the new 2,2'-bidipyrin ligands **1** and **2** is illustrated in Scheme 1. We have chosen an eight-membered ring as an intermediately severe constraint for our purpose. A bis(indole)-based N₄ ligand with an identical restraint was prepared and studied before in the field of anion sensing,^[15] and a maximum bis(indole) torsion angle of 65° was estimated for this compound. This estimate fits well for our intention to produce a 2,2'-bidipyrin with a restriction to the *syn*- and/or *syn-gauche* conformation.



Scheme 1. Preparation of restrained 2,2'-bidipyrins **1** and **2** as bis(hydroperchlorate) salts.

The new ligands **1** and **2** were obtained analogously to simpler 2,2'-bidipyrins recently described.^[11c,11d] Dialdehyde **5** was prepared from the recently communicated diester **3**^[16] by a saponification-decarboxylation-formylation sequence. The electron-rich bipyrrole **4** proved to be ex-

remely sensitive to light and air, and was therefore used directly in the Vilsmeier formylation to yield **5** as a yellow powder in an overall yield of 72%. The acid-promoted double condensation of **5** with 2 equiv. of a 5-unsubstituted pyrrole (either **6** or **7**) was carried out at 60 °C in methanol solution. Perchloric acid was found to be the agent of choice, as the protonated products **1**·2 HClO₄ and **2**·2 HClO₄ directly crystallize from the hot reaction mixture. The yields of 50 and 48%, however, are significantly lower compared to the almost quantitative formation of nonhindered 2,2'-bidipyrins.

The formation of the desired tetrapyrroles **1** and **2** is indicated mass spectrometrically by the signals for the [M + 1]⁺ ions at *m/z* 481 and 537, respectively. Combustion analyses in combination with thermogravimetric investigations point to the presence of hydrates, that is [1·2HClO₄·H₂O] and [2·2HClO₄·3H₂O]. Further characterization was performed by ¹H and ¹³C NMR spectroscopy. Proton NMR spectra of [1·2HClO₄·H₂O] and [2·2HClO₄·3H₂O] show broad singlets for two types of NH protons at 12.23 and 11.47 (**1**) or 11.17 and 10.55 ppm (**2**) in addition to a sharp resonance line for the *meso* H atoms at 7.06 (**1**) or 7.25 ppm (**2**). The singlet for the terminal methyl groups is found at 2.76 (**1**) and 2.73 ppm (**2**), and the C₄-bridge leads to broadened multiplets for the benzylic and homobenzylic methylene protons at δ = 2.7 and 1.8 ppm, respectively (Figure 3).

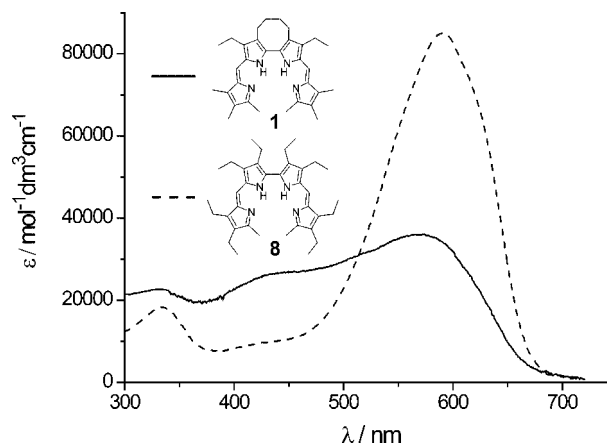
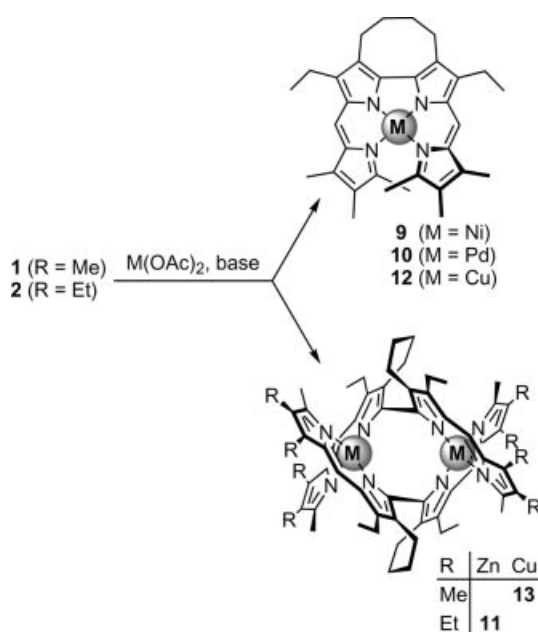


Figure 3. UV/Vis spectra (CH₂Cl₂) of free base **1** and octaethyldimethyl-2,2'-bidipyrin **8**.^[11d]

While the data discussed above give no direct hint to a special conformation of the new tetrapyrroles, the restricted rotation of **1** and **2** is well documented in the optical spectra. Figure 3 shows the UV/Vis absorption spectra of restrained **1** and of the unrestrained 2,2'-bidipyrin **8**.^[11d] Compared to octaethyldimethyl-2,2'-bidipyrin **8** the optical transitions of **1** are significantly broader and largely equal in intensity, but very similar with respect to the absorption maxima. A possible interpretation of this spectral pattern is that the presence of the eight-membered ring in **1** prevents a single minimum conformation for the tetrapyrrole in solution. Instead, a number of energetically similar *syn-gauche* conformations exist and slowly interconvert into

each other. The observed line-broadening for the C₄-bridge methylene proton signals in the ¹H NMR spectra of **1** and **2** as well as the relatively high solubility of the new tetrapyrroles provide additional support for this thesis. An attempt to investigate this issue further by variable temperature NMR spectroscopy on **1** failed, however, because of severely overlapping resonances in the aliphatic region.

Metal coordination was studied using divalent metal acetates and excess base (sodium acetate, ammonia or sodium methoxide) in methanolic solution. Only zinc(II), copper(II), nickel(II) and palladium(II) yielded isolable complexes with **1** or **2** while no binding was observed for iron(II), manganese(II) and vanadyl(IV), and only decomposition products were detected after treatment with cobalt(II) acetate. The successful attempts are summarized in Scheme 2.



Scheme 2. Formation of nickel(II), palladium(II), zinc(II) and copper(II) chelates **9–13** from rotationally restricted 2,2'-bidipyrins **1** and **2**.

The formation of nickel and palladium chelates **9** and **10** is easily monitored by an immediate colour change from dark green to brownish green and red, respectively, upon addition of metal acetate and sodium acetate to a solution of **1**. Isolation can be effected in good yields after chromatographic workup and recrystallization. As expected, the new complexes are of type **A** with a distorted square-planar arrangement of the *N* donors and therefore analogous to known nonbridged nickel- and palladium-2,2'-bidipyrins of, for example, **8**.^[12c,12d] Results from high-resolution mass spectrometry, NMR spectroscopy and UV/Vis measurements further support the assignments. In particular, the small high-field shift for the terminal methyl proton resonances at 2.44 (**9**) and 2.57 ppm (**10**) is a good indication for the strain, which is typically present at this position in helical dimethyl-2,2'-bidipyrins of type **A**. In addition, the resonances of the *meso* protons are also detected high-field

shifted at 6.24 (**9**) and 6.40 ppm (**10**). Unlike for the protonated **1** and **2**, the signals for the methylene protons of the C₄ bridge show sharp absorptions and indicate a rigid conformation of the eight-membered ring. The optical spectra of the nickel and palladium chelates **9** and **10** show two major absorptions at 430/530 or 430/520 nm, respectively, and are almost indistinguishable from those of their unrestrained analogues with ligand **8** (Figure 4).^[12c,12d]

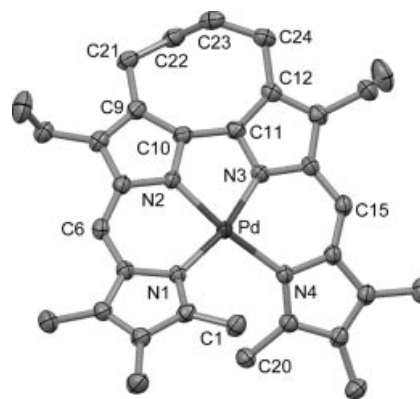


Figure 4. Molecular structure of **10**. Ellipsoids are set at 50% probability (hydrogen atoms omitted for clarity).

A detailed picture of the coordination and the degree of molecular distortion was derived from X-ray crystallographic work performed on the palladium derivative **10**. Suitable crystals were obtained by slow evaporation of a solution of **10** in dichloromethane/*n*-hexane. The compound crystallizes monoclinically in the space group *P2₁/n* and forms green metallic plates. The molecular structure of **10** is given in Figure 4. Table 1 summarizes selected angles and distances.

The palladium(II) ion is coordinated to the four nitrogen donors of the 2,2'-bidipyrin in a distorted square-planar fashion with Pd–N distances of 1.963(2)–2.071(2) Å. The *in-plane* distortion is mainly due to the presence of the bipyrolic subunit, which allows an N2–Pd–N3 angle of only 78.32(9)°. More interestingly, the *out-of-plane* distortion caused by the close proximity of the terminal methyl groups C1 and C20 can be analyzed using different torsion angles. Values relevant for comparison are the torsion angles N2–C9–C10–N3, C8–C9–C10–C11 and C2–C10–C11–C19, which are found to be 11.8(3), 27.3(6) and 21.4(1)°, respectively, in **10**. These angles are reduced by 4.7, 7.3 and 6.3° with respect to the unconstrained Pd^{II} chelate from ligand **8** and, in combination with the shorter C1–C20 distance of 3.217(4) Å (3.473 Å for Pd-**8**), a slight planarization of **10** becomes visible. The differences between the solid-state structures of **10** and the literature precedent, however, are quite small. In both cases the distances between the terminal methyl groups clearly undercut the sum of the *van der Waals* distances and prove the strained situation at these positions. The annelated eight-membered ring of **10** itself resides in a twist conformation, and no disorder is found in the crystal at this position (Figure 5).

The preparation of the zinc chelate **11** is straightforward. The action of sodium methoxide and excess zinc acetate on

Table 1. Selected structural data for **10**, **11** and **13**.^[a]

Compound	10			11		13		
	Pd	Zn-Ia ^[b]	Zn-Ib ^[b]	Zn-IIa ^[b]	Zn-IIb ^[b]	Cu-Ia ^[b]	Cu-Ib ^[b]	Cu-II ^[b]
N1–M	2.060(2)	2.004(3)	2.002(3)	2.009(3)	2.017(3)	2.005(6)	1.971(5)	1.983(6)
N2–M	1.963(2)	1.995(3)	2.001(3)	1.987(3)	1.992(3)	1.947(5)	1.942(6)	1.939(6)
N3–M	1.964(2)	1.974(3)	1.986(3)	1.992(3)	1.992(3)	1.951(6)	1.938(5)	1.969(5)
N4–M	2.071(2)	2.030(4)	2.024(3)	2.001(3)	1.988(3)	1.996(6)	2.001(6)	1.999(6)
C5–C6	1.382(4)	1.373(5)	1.365(5)	1.374(8)	1.372(4)	1.394(13)	1.366(13)	1.374(13)
C6–C7	1.397(4)	1.389(6)	1.395(5)	1.394(9)	1.386(4)	1.394(11)	1.400(12)	1.400(12)
C10–C11	1.458(4)	1.443(6)	1.446(6)	1.439(6)	1.441(6)	1.457(11)	1.433(11)	1.436(11)
C14–C15	1.400(4)	1.435(8)	1.398(6)	1.401(6)	1.388(7)	1.401(11)	1.383(11)	1.385(11)
C15–C16	1.382(4)	1.356(8)	1.378(6)	1.361(6)	1.357(8)	1.375(11)	1.362(11)	1.378(11)
C9–C21	1.500(4)	1.508(7)	1.512(6)	1.485(19)	1.511(6)	1.503(13)	1.50(5)	1.489(13)
C21–C22	1.517(4)	1.517(9)	1.488(10)	1.496(12)	1.523(8)	1.50(2)	1.50(5)	1.528(13)
C22–C23	1.533(4)	1.498(12)	1.541(16)	1.500(13)	1.508(10)	1.44(3)	1.51(4)	1.516(14)
C23–C24	1.512(4)	1.497(13)	1.363(14)	1.467(11)	1.481(11)	1.499(19)	1.378(18)	1.504(14)
C24–C12	1.508(4)	1.483(11)	1.498(7)	1.561(8)	1.519(8)	1.512(11)	1.508(13)	1.512(10)
M···M'	–	3.4427(7)		3.3579(7)		3.0629(13)		3.0123(13)
$\Delta(1,2,6)^{[c]}$	0.5386(2)	0.1942(4)	0.2450(4)	0.1306(4)	0.1119(4)	0.0929(9)	0.0622(9)	0.0363(9)
$\Delta(3,4,15)^{[c]}$	0.4796(2)	0.1519(4)	0.1385(4)	0.1055(4)	0.1253(4)	0.0167(9)	0.0460(9)	0.0252(9)
N1–M–N2	88.78(9)	93.50(12)	94.11(12)	95.19(13)	93.50(12)	94.1(2)	93.8(2)	92.3(2)
N1–M–N3	164.93(9)	118.83(12)	117.14(13)	106.76(12)	114.25(12)	104.5(3)	101.1(2)	104.5(2)
N1–M–N4	104.52(8)	122.13(12)	119.97(14)	119.18(13)	121.63(13)	122.7(2)	127.5(3)	125.9(2)
N2–M–N3	78.32(9)	127.47(12)	129.75(13)	130.24(13)	131.78(14)	144.4(3)	141.2(3)	143.7(3)
N2–M–N4	164.54(9)	102.72(13)	103.31(13)	113.39(12)	104.87(15)	102.6(2)	105.6(3)	102.5(3)
N3–M–N4	89.41(8)	93.80(13)	94.10(15)	94.11(11)	93.39(15)	92.7(2)	93.4(2)	93.3(2)
C5–C6–C7	127.5(2)	129.5(4)	129.5(4)	130.4(4)	129.2(3)	128.6(7)	130.5(7)	127.4(7)
C14–C15–C16	127.8(2)	129.2(4)	131.0(5)	128.8(4)	129.6(4)	127.8(7)	129.1(7)	128.8(7)
C9–C21–C22	114.3(2)	113.7(4)	115.3(5)	118.9(6)	111.9(4)	113.1(10)	129(4)	116.4(8)
C21–C22–C23	112.8(2)	116.9(6)	118.7(7)	118.8(7)	114.5(5)	117.7(15)	132(4)	117.2(8)
C22–C23–C24	112.9(2)	123.9(8)	113.2(9)	117.6(6)	118.2(7)	120.6(14)	124(2)	118.9(9)
C23–C24–C12	114.1(2)	119.9(6)	124.9(7)	114.3(5)	117.2(5)	121.1(10)	117.2(11)	117.4(8)
N2–C10–C11–N3	11.8(3)	41.3(6)	39.9(5)	38.4(6)	37.9(6)	38.4(12)	40.0(12)	41.1(10)
C9–C10–C11–C12	27.3(6)	52.4(8)	51.0(7)	47.1(8)	48.0(8)	51.5(14)	54.9(16)	53.4(13)
C21–C22–C23–C24	131.1(2)	63.3(10)	75.6(11)	64.4(11)	57.6(7)	72(2)	51(5)	74.5(13)

[a] Unified numbering scheme used for all compounds, see Figure 5. [b] I and II correspond to crystallographically distinct helicates, a and b determine the respective BDP in each dimer. [c] Out-of-plane distance of the metal ion from the N1–N2–C6 or N3–N4–C15 plane.

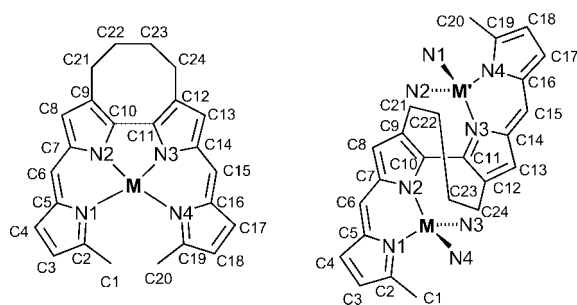


Figure 5. Unified numbering scheme used for the complexes and/or single-strand fragments of **10**, **11** and **13** in Figures 4, 6, 7, 9 and 10, and in Table 1.

ligand **2** in methanolic solution results in an immediate colour change from dark to light green. Because of the high solubility of the product **11** in most organic solvents the new complex can conveniently be isolated from this mixture by repeated pentane extraction, and forms green plates after crystallization. The results from mass spectrometry clearly point to the formation of a dinuclear zinc complex of type **C** with a complicated isotope pattern around m/z 1200. Proton NMR shows the formation of a symmetric compound,

in which the terminal methyl proton signal is strongly shifted to high field with respect to **2** and can be observed as a singlet at $\delta = 1.66$ ppm. The signal for the *meso* protons, however, appears at $\delta = 6.95$ ppm without any significant shift (Figure 6).

For further characterization an X-ray crystallographic analysis was performed on **11**. Suitable green plates were obtained by slow evaporation of a solution of **11** in dichloromethane/*n*-hexane (1:3). Complex **11** crystallizes in the triclinic space group $P\bar{1}$. Two independent molecules I and II and their respective enantiomers are found in the unit cell. Multiple disorder was found for the orientation of nine ethyl substituents, which had to be refined with restraints. In addition, three of the four C_4 bridges are found to be strongly disordered and were refined assuming two conformations with occupancy factors for the atoms of concern of 0.5. Only data of molecule I will be discussed. Data for molecule II, however, are presented in Table 1 for comparison. The molecular structure of **11-I** is depicted in Figure 6. For the numbering scheme, see Figure 5.

The molecular structure of **11** shows a dinuclear double-stranded helicate with the zinc ions embedded in four N donor centres with a distorted tetrahedral geometry. Each zinc ion is coordinated to two N donor atoms of each 2,2'-

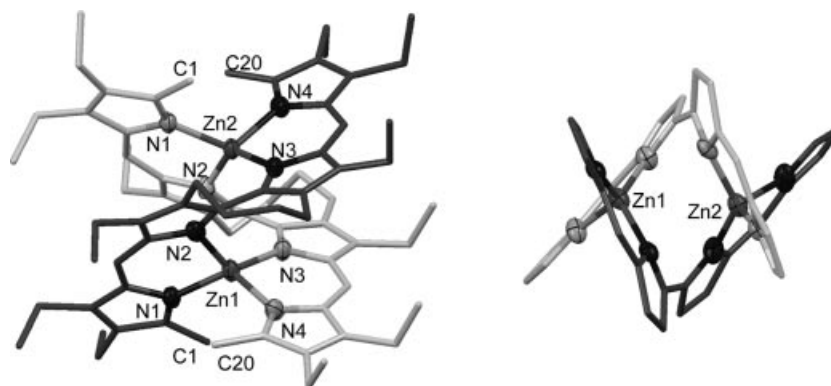


Figure 6. Molecular structure of **11**. Left side: *P* enantiomer of molecule I (carbon atoms as capped sticks and hydrogen atoms omitted for clarity); right side: view of the coordination environments of the zinc ions (alkyl substituents and hydrogen atoms removed). Ellipsoids are set at 40% probability.

bidipyrin ligand. To allow the binding of two zinc centres to the same ligand the tetrapyrrole has to rotate around the central pyrrole–pyrrole bond C10–C11. The torsion at this position is, however, restricted to 41.3(6)/39.9(5) and 52.4(8)/51.0(7)° [N2–C10–C11–N3 and C9–C10–C11–C12 for the two strands of molecule I, respectively] by the annelated-eight membered ring, so that the ligand resides in the *syn-gauche* conformation with compressed ZnN₄ units. In the literature precedent of a nonrestrained dinuclear bidipyrinato-helicate of zinc^[7b] respective torsion angles are as large as 112.3 and 108.8° and indicate an *anti-gauche* conformation of the tetrapyrrole. The compression of the tetrahedral binding environment of the zinc ions in **11** can best be viewed by the dihedral angles between N1–Zn–N2 and N3–Zn–N4 planes, which should be 90° for a tetrahedron but range from 75.8 to 80.9° for **11**. The unrestrained ana-

logue, on the other hand, shows an enlarged dihedral angle of 102.0°. The Zn–N distances of **11** [1.974(3)–2.030(4) Å] and the literature precedent (1.982–1.996 Å) do not differ much, but the zinc···zinc distance of **11** shrinks dramatically from 4.891 Å to 3.443 Å as a result of the backbone constraint. It should be noticed that the eight-membered rings do not form a single low-energy conformer but are found to reside either in a twist or boat conformation.^[17]

The helicates of **11** arrange in pillars, which propagate along the crystallographic *b* axis (Figure 7). Next neighbours within these pillars are always of a different structure (i.e., molecule I next to molecule II and vice versa), and are alternately 10.116 and 10.149 Å apart from each other. With respect to the stereochemistry of the helicates, it is remarkable that only one enantiomeric form is contained in each chain, thus forming chiral *M*- or *P*-helical pillars. Heli-

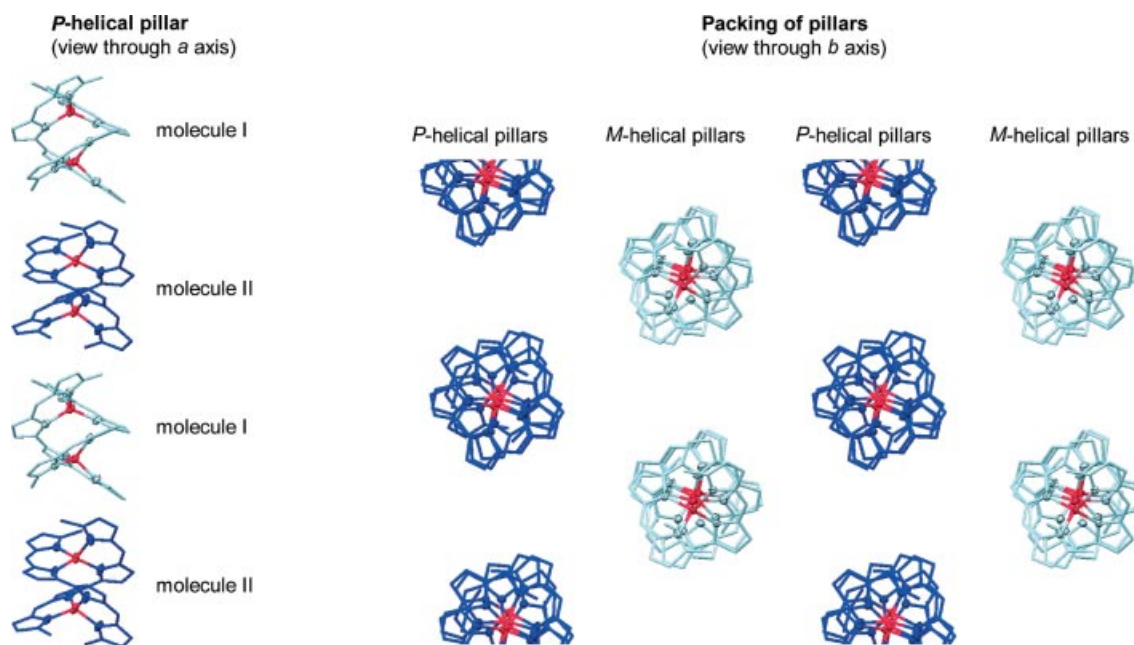


Figure 7. Packing of **11** in the crystal. Left side: *P*-helical pillar formed by the alternating arrangement of *P*-helical isomers of molecules I (bright) and II (dark). Right side: view along the pillars propagating in the crystallographic *b* axis (*P*-helices dark, *M*-helices bright). The ellipsoids are set at 40% probability. Alkyl side chains and hydrogen atoms removed for clarity.

cal pillars with both senses are then densely packed in the crystal as shown on the right in Figure 7.

Copper complexes of 2,2'-bidipyrins usually form either in the type **A** or the type **C** structure, depending on the reaction conditions.^[11f,12c] In this case, the outcome of the reaction of **1** and copper acetate depends critically on the choice of the added base. If concentrated ammonia is added to a mixture of **1** and excess copper(II) acetate in methanol, only the immediate formation of a brownish-red monomeric species **12** of type **A** is observed. Using sodium methoxide results in a mixture of **12** and some green dimeric species **13** of type **C**, which becomes the major component if only sodium acetate is added to absorb the released protons. In either case, however, the separation and isolation of **12** and **13** is quite simple because of their large differences in solubility. Monomeric **12** tends to crystallize almost quantitatively from methanolic solutions (up to 65% yield), while **13** is soluble even in cold pentane and can thus be conveniently extracted from the reaction mixtures and isolated in up to 54% yield. The compositions of both compounds were confirmed by combustion analysis and mass spectrometry.

EPR spectroscopy shows the expected signal for **12** in dichloromethane solution at ambient temperature with $g_{\text{iso}} = 2.096$ and a quartet with $A_{\text{Cu}} = 82.1$ G. This spectrum is

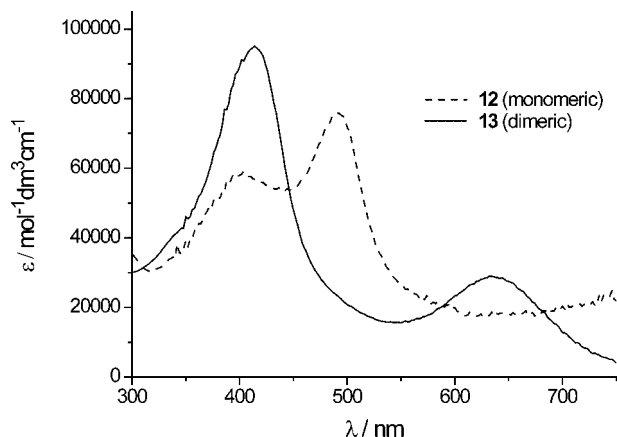


Figure 8. UV/Vis spectra (CH_2Cl_2 , 293 K) of monomeric and dimeric copper(II) chelates **12** and **13**.

identical to the one described before for the copper chelate of the unrestrained ligand **8**.^[12c] Complex **13**, on the other hand, is EPR-silent under these conditions. As no well-resolved ^1H NMR spectrum was observed, we conclude that the Cu^{II} atoms of **13** are weakly antiferromagnetically coupled. The UV/Vis spectra of **12** and **13** are shown in Figure 8. Both are clearly governed by the $\pi\text{--}\pi^*$ transitions of their 2,2'-bidipyrin ligands, which obviously change with different conformations.

An X-ray crystallographic analysis shows that **13** resides in the assumed bis-helical structure. The complex crystallized by slow evaporation of a solution of **13** in dichloromethane/pentane as a solvate $\text{13} \cdot \frac{1}{3}\text{C}_5\text{H}_{12}$ in the orthorhombic system, space group $Pbcn$. Two independent molecules I and II and their respective enantiomers are found in the unit cell. Crystallographically molecule II as well as the solvent are situated on inversion centres, which explains the formula of the solvate. The eight-membered rings of molecule I and the solvent are disordered. Because of the severity of the disorder the solvent molecule was treated with the SQUEEZE command in Platon. The disorder of the eight-membered rings of molecule I is very severe, and the most disordered methylene groups had to be refined in two positions with occupancy factors of 0.5 (C22, C23) and 0.8422/0.1578 (C53, C54) and with additional restraints. Only the molecular parameters of molecule II (Figure 9) will be discussed further. Data for both molecules are presented in Table 1.

As for the zinc complex **11** shown above, the copper atoms of **13** are coordinated to both tetrapyrrole strands, which reside in a *syn-gauche* conformation with N2--C10--C11--N3 and C9--C10--C11--C12 torsion angles of $41.1(10)$ and $53.4(13)^\circ$, respectively, in order to accommodate two transition-metal ions. The copper N_4 coordination is again that of a compressed tetrahedron, which shows Cu--N bond lengths of $1.939(6)\text{--}1.999(6)$ Å and angles between the N1--Cu--N2 and N3--Cu--N4 planes of 65.18° , even smaller than those seen in **11**. The two copper(II) ions are located only $3.0123(13)$ Å apart from each other, so that a noticeable antiferromagnetic exchange interaction can be expected. This finding is in agreement with the EPR-silent character of **13**.

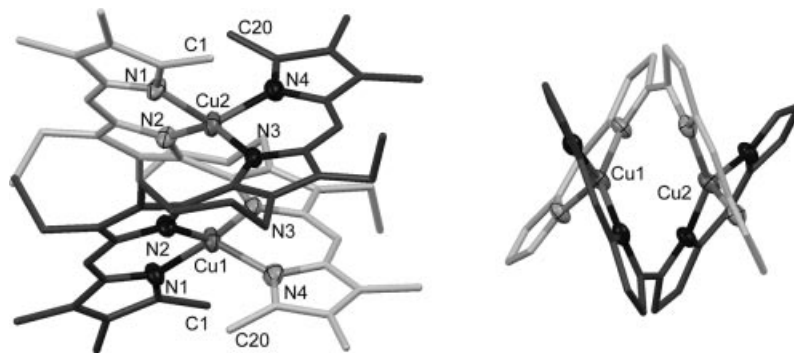


Figure 9. Molecular structure of **13**. Left side: *P* enantiomer of molecule II (carbon atoms as capped sticks and hydrogen atoms omitted for clarity); right side: view of the coordination environments of the copper ions (alkyl substituents and hydrogen atoms removed). Ellipsoids are set at 40% probability.

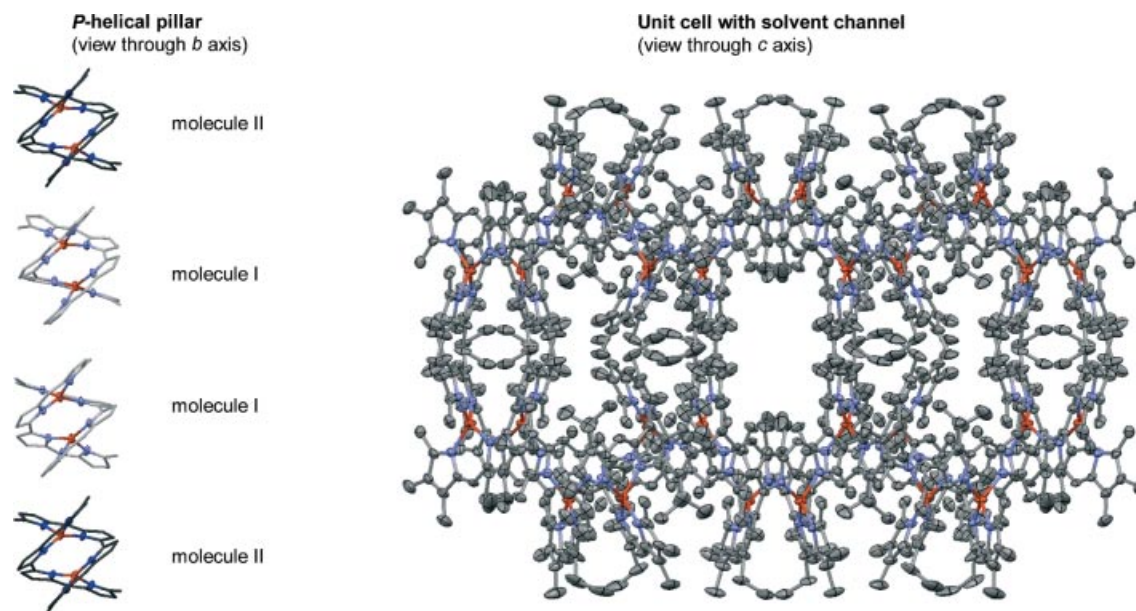


Figure 10. Packing of **13** in the crystal. Left side: *P*-helical pillar formed by *P*-helical isomers of molecule I (bright) and II (dark). Alkyl side chains and hydrogen atoms are removed for clarity. Right side: View down the solvent channel along the crystallographic *c* axis of the unit cell of **13** (solvent removed). The ellipsoids are set at 40% probability. Hydrogen atoms were removed for clarity.

The similarity between the solid-state structures of **11** and **13** comprises even the formation of enantiopure helical pillars from 1D strands of individual molecules, which are found along the crystallographic *a* axis in the crystal of **13**. The molecules are arranged in alternating distances of 9.628 and 11.124 Å (Figure 10). The obvious deviations of the packing pattern, however, originate from the differing sequences of molecules I and II within these strands, which are I – II – I – II for **11** but I – I – II – I – I – II for **13**. This nonalternating mode of the latter opens inner channels along the *c* axis (right in Figure 10), which are filled with disordered solvent molecules in order to stabilize the crystal lattice.

Conclusions

In summary, we have prepared the first examples of conformationally restricted 2,2'-bidipyrriins **1** and **2** and described syntheses, spectroscopic properties and structural investigations for several transition-metal complexes of type **A** and type **C**. Concerning the coordination modes and binding abilities for different transition-metal ions, the constrained 2,2'-bidipyrriins **1** and **2** are amazingly similar to the unconstrained ones like **8**, although conformational differences in the molecular fine-tune have been shown by the crystallographic analyses. The aim of stabilizing labile ions in the 2,2'-bidipyririn environment could not be achieved by this approach. However, structural information on dinuclear copper chelates of tetrapyrrolic ligands was obtained for the first time, and the unexpected finding of enantiopure 1D helical pillars for dinuclear complexes with short M...M distances points to further investigations into the use of such restricted ligands for anisotropic materials, metal-organic frameworks (MOFs) and the like.

Experimental Section

General: All reagents and solvents were purchased from commercial sources and used as received. Bipyrrole diester **3**,^[16] trimethylpyrrole **6**^[18] and diethylmethylpyrrole **7**^[19] were prepared as previously reported. NMR spectra were obtained with a Bruker AMX 400 spectrometer in the solvents indicated below. EPR spectra were measured with a Bruker ESP 300 instrument at X-band. Mass spectra were recorded with a Finnigan 90 MAT or a Micromass AutoSpec instrument. *m/z* values are given for the most abundant isotopes only. UV/Vis spectra were measured with a Hitachi U-3200 in the range 300–800 nm. Melting points were determined by DTA with a Thermoanalyzer DuPont 9000. For X-ray crystallographic measurements a Bruker Smart Apex with D8 goniometer was used.

CCDC-271753 to -271755 contain the supplementary crystallographic data for this paper. These data can be obtained free of charge from The Cambridge Crystallographic Data Centre via www.ccdc.cam.ac.uk/data_request/cif.

Synthesis of 3,3'-(1,4-Butanediyl)-4,4'-diethyl-2,2'-bipyrrole-5,5'-dicarbaldehyde (5**):** The bipyrrole diester **3** (6.95 g, 18.0 mmol) and sodium hydroxide (1.45 g, 36.0 mmol) were mixed with ethylene glycol (120 mL) and heated to reflux with good stirring and under strict exclusion of dioxygen and light for 2 h. Upon cooling in ice, a yellow, light-sensitive solid started to form. Degassed ice water (90 mL) was added dropwise at this temperature, and the solid was filtered, washed with additional water, and dried in the dark in high vacuo. The material was then dissolved in DMF (100 mL) with exclusion of air and moisture and cooled to 0 °C. At this temperature phosphoryl chloride (3.80 mL, 41.0 mmol) was added dropwise. Ten minutes after the addition, cooling was stopped and the mixture stirred at ambient temperature for another 2 h. The mixture was poured into water (400 mL) in an open flask, and a solution of sodium hydroxide in water (30%) was added, until a solid formed. This solid was filtered, washed carefully with water and dried in high vacuo to yield the title compound as a yellow powder. Yield 3.86 g (82%). M.p. 130 °C. ¹H NMR (400 MHz, CDCl₃, 25 °C): δ = 1.22 (t, 6 H, *J* = 7.3 Hz, CH₃CH₂pyr), 1.81 (br. s, 4 H,

$\text{CH}_2\text{CH}_2\text{pyr}$), 2.75–2.70 (m, 8 H, $\text{CH}_2\text{CH}_2\text{pyr}$ and $\text{CH}_3\text{CH}_2\text{pyr}$), 9.65 (br. s, 2 H, CHO), 11.56 (br. s, 2 H, NH) ppm. $^{13}\text{C}\{^1\text{H}\}$ NMR (100 MHz, CDCl_3 , 25 °C): δ = 17.0, 17.1, 21.9, 26.5, 124.4, 129.3, 130.0, 138.9, 177.4 ppm. HRMS (ESI) calcd. for $\text{C}_{18}\text{H}_{22}\text{N}_2\text{O}_2$: 298.1681; obsd. 298.1672, Δ = 0.9 mmu. $\text{C}_{18}\text{H}_{22}\text{N}_2\text{O}_2$ (298.38): calcd. C 72.46, H 7.43, N 9.39; found C 72.39, H 7.26, N 9.45.

Synthesis of 3,3'-(1,4-Butanediyl)-4,4'-diethyl-8,8',9,9',10,10'-hexamethyl-2,2'-bidipyrin (1) as Bis(hydropchlorate): A suspension of **5** (100 mg, 0.33 mmol) and 2,3,4-trimethylpyrrole (**6**) (80 mg, 0.74 mmol) in methanol (5 mL) was heated to 60 °C. At this temperature perchloric acid (1 mL of a 70% solution in water) was added at once and heating was discontinued. The colour of the mixture changed immediately to dark green. The product crystallized upon cooling in ice as a dark solid, which was filtered, washed with small portions of ice-cold methanol, and dried in vacuo to yield a green solid. Yield 123 mg (50%). M.p. 151 °C (dec.). ^1H NMR (400 MHz, CDCl_3 , 25 °C): δ = 1.19 (t, 6 H, J = 7.3 Hz, $\text{CH}_3\text{CH}_2\text{pyr}$), 1.80 (m, 4 H, $\text{CH}_2\text{CH}_2\text{pyr}$), 2.00, 2.25 (2 \times s, 12 H, 2 \times CH_3pyr), 2.58–2.73 (m, 8 H, $\text{CH}_2\text{CH}_2\text{pyr}$ and $\text{CH}_3\text{CH}_2\text{pyr}$), 2.76 (s, 6 H, *term*- CH_3), 7.06 (s, 2 H, *meso*-H), 11.47 (br. s, 2 H, NH), 12.23 (br. s, 2 H, NH) ppm. $^{13}\text{C}\{^1\text{H}\}$ NMR (100 MHz, CDCl_3 , 25 °C): δ = 9.2, 10.4, 14.0, 16.2, 18.2, 22.6, 26.1, 118.9, 127.7, 128.9, 129.6, 131.7, 137.1, 143.5, 144.9, 161.7 ppm. MS (FAB): 481 $[\text{M} - (\text{HCl}_2\text{O}_8)]^+$. UV/Vis (CH_2Cl_2): λ_{max} (ϵ , $\text{L mol}^{-1}\text{cm}^{-1}$) = 330 (23000), 435 (27000), 565 (36000) nm. $\text{C}_{32}\text{H}_{42}\text{Cl}_2\text{N}_4\text{O}_8\cdot 3\text{H}_2\text{O}$ (735.649): calcd. C 52.25, H 6.58, N 7.62; found C 52.39, H 6.56, N 7.85.

Synthesis of 3,3'-(1,4-Butanediyl)-4,4',8,8',9,9'-hexaethyl-10,10'-dimethyl-2,2'-bidipyrin (2) as Bis(hydropchlorate): Complex **2** was prepared from **3** (100 mg, 0.33 mmol) and 3,4-diethyl-2-methylpyrrole (**7**) (100 mg, 0.74 mmol) as described above for **1** and yielded a brown-violet powder. Yield 128 mg (48%). M.p. 236 °C (dec.). ^1H NMR (400 MHz, CD_2Cl_2 , 25 °C): δ = 1.17, 1.25, 1.27 (6 \times t, 18 H, J = 7.3 Hz, $\text{CH}_3\text{CH}_2\text{pyr}$), 1.86 (m, 4 H, $\text{CH}_2\text{CH}_2\text{pyr}$), 2.54 (q, 4 H, J = 7.3 Hz, $\text{CH}_3\text{CH}_2\text{pyr}$), 2.68–2.82 (m, 12 H, $\text{CH}_2\text{CH}_2\text{pyr}$ and $\text{CH}_3\text{CH}_2\text{pyr}$), 2.73 (s, 6 H, *term*- CH_3), 7.25 (s, 2 H, *meso*-H), 10.55 (br. s, 2 H, NH), 11.17 (br. s, 2 H, NH) ppm. $^{13}\text{C}\{^1\text{H}\}$ NMR (100 MHz, CD_2Cl_2 , 25 °C): δ = 13.7, 14.4, 15.9, 16.6, 17.0, 17.4, 18.4, 22.6, 26.2, 119.2, 129.3, 130.4, 131.3, 133.8, 137.2, 145.8, 150.4, 162.5 ppm. MS (FAB): 537 $[\text{M} - (\text{HCl}_2\text{O}_8)]^+$. UV/Vis (CH_2Cl_2): λ_{max} (ϵ , $\text{L mol}^{-1}\text{cm}^{-1}$) = 330 (24000), 430 (27000), 565 (37000) nm. $\text{C}_{36}\text{H}_{50}\text{Cl}_2\text{N}_4\text{O}_8\cdot \text{H}_2\text{O}$ (755.725): calcd. C 57.22, H 6.94, N 7.41; found C 57.35, H 6.66, N 7.42.

Synthesis of 3,3'-(1,4-Butanediyl)-4,4'-diethyl-8,8',9,9',10,10'-hexamethyl-2,2'-bidipyrinatonicel(II) (9): A solution of nickel acetate tetrahydrate (50 mg, 0.20 mmol) in methanol (3 mL) was added to a suspension of **1** (100 mg, 0.15 mmol) and sodium acetate (100 mg, 1.21 mmol) in methanol (10 mL) and the resulting mixture was stirred for 30 min at ambient temperature. The solvent was removed in vacuo, and the residue was purified by silica chromatography with dichloromethane/*n*-hexane (1:1). The greenish-brown fraction was collected and the solvent was removed to yield **9** as a violet solid. Yield 44 mg (54%). M.p. 239 °C. ^1H NMR (400 MHz, C_6D_6 , 25 °C): δ = 1.10 (t, 6 H, J = 7.3 Hz, $\text{CH}_3\text{CH}_2\text{pyr}$), 1.39 (s, 6 H, CH_3pyr), 1.58–1.54 (m, 2 H, $\text{CH}_2\text{CH}_2\text{pyr}$), 1.66 (s, 6 H, CH_3pyr), 1.85–1.75 (m, 2 H, $\text{CH}_2\text{CH}_2\text{pyr}$), 2.20–2.52 (m, 8 H, $\text{CH}_2\text{CH}_2\text{pyr}$ and $\text{CH}_3\text{CH}_2\text{pyr}$), 2.44 (s, 6 H, *term*- CH_3), 6.24 (s, 2 H, *meso*-H) ppm. $^{13}\text{C}\{^1\text{H}\}$ NMR (100 MHz, C_6D_6 , 25 °C): δ = 9.3, 9.7, 16.3, 17.9, 18.4, 25.2, 26.6, 120.2, 125.1, 126.2, 133.8, 138.8, 140.8, 141.9, 152.1, 168.4 ppm. HRMS (ESI) calcd. for $\text{C}_{32}\text{H}_{38}\text{N}_4\text{Ni}$: 536.24498; obsd. 536.24629, Δ = 1.31 mmu. UV/Vis (CH_2Cl_2): λ_{max} (ϵ , $\text{L mol}^{-1}\text{cm}^{-1}$) = 350 (20000), 430 (81000), 530

(18000), 610sh (12000) nm. $\text{C}_{32}\text{H}_{38}\text{N}_4\text{Ni}$ (537.364): calcd. C 71.52, H 7.13, N 10.43; found C 71.13, H 6.96, N 10.09.

Synthesis of 3,3'-(1,4-Butanediyl)-4,4'-diethyl-8,8',9,9',10,10'-hexamethyl-2,2'-bidipyrinatopalladium(II) (10): A solution of palladium acetate (59 mg, 0.26 mmol) in methanol (5 mL) was added to a suspension of **1** (180 mg, 0.26 mmol) and sodium acetate (100 mg, 1.21 mmol) in methanol (10 mL) and the resulting mixture was stirred for 30 min at ambient temperature. The solvent was removed in vacuo, and the residue was purified by radial chromatography on silica with dichloromethane/*n*-hexane (1:1). The deep red fraction was collected, the solvent was removed and the residue was recrystallized from dichloromethane/*n*-hexane (1:2) to yield **10** as brownish-red crystals. Yield 94.0 mg (62%). M.p. 202 °C. ^1H NMR (400 MHz, C_6D_6 , 25 °C): δ = 1.12 (t, 6 H, J = 7.3 Hz, $\text{CH}_3\text{CH}_2\text{pyr}$), 1.52 (s, 6 H, CH_3pyr), 1.71–1.75 (m, 2 H, $\text{CH}_2\text{CH}_2\text{pyr}$), 1.77 (s, 6 H, CH_3pyr), 1.81–1.86 (m, 2 H, $\text{CH}_2\text{CH}_2\text{pyr}$), 2.35–2.41 (m, 6 H, $\text{CH}_2\text{CH}_2\text{pyr}$ and $\text{CH}_3\text{CH}_2\text{pyr}$), 2.54–2.61 (m, 2 H, $\text{CH}_2\text{CH}_2\text{pyr}$), 2.57 (s, 6 H, *term*- CH_3), 6.40 (s, 2 H, *meso*-H) ppm. $^{13}\text{C}\{^1\text{H}\}$ NMR (100 MHz, C_6D_6 , 25 °C): δ = 9.6, 9.9, 16.8, 17.0, 18.1, 22.7, 27.6, 120.6, 124.8, 126.8, 132.4, 138.1, 138.2, 142.0, 151.6, 165.4 ppm. HRMS (ESI) calcd. for $\text{C}_{32}\text{H}_{38}\text{N}_4\text{Pd}$: 584.21311; obsd. 584.21205, Δ = 1.06 mmu. UV/Vis (CH_2Cl_2): λ_{max} (ϵ , $\text{L mol}^{-1}\text{cm}^{-1}$) = 430 (82000), 520 (32000), 770 (11000) nm. $\text{C}_{32}\text{H}_{38}\text{N}_4\text{Pd}$ (585.09): calcd. C 65.69, H 6.55, N 9.58; found C 65.42, H 6.41, N 9.37.

Crystallographic Data for 10: $\text{C}_{32}\text{H}_{38}\text{N}_4\text{Pd}$, green plates obtained by slow concentration of a CH_2Cl_2 /*n*-hexane solution, crystal size: $0.40 \times 0.40 \times 0.30$ mm, monoclinic, space group $P2_1/n$, a = 8.8497(10), b = 24.160(3), c = 12.8685(14) Å, β = 98.421(2)°, V = 2721.7(5) Å³, $\rho_{\text{calcd.}}$ = 1.428 g cm^{−3}, Z = 4, $2\theta_{\text{max}}$ = 50°, Mo- K_{α} radiation, λ = 0.71073 Å, scan mode: ω -scans, T = 193(2) K, 31431 measured, 4798 independent reflections, 4620 reflections observed for $I > 2\sigma(I)$, μ = 0.710 mm^{−1}, solved by Patterson method, refined with full-matrix least-squares on F^2 [20], 342 parameters, H atoms refined with isotropic temperature factors. R = 0.0340, wR = 0.0821, residual electron density ρ = 0.730/−0.313 e Å^{−3}.

Bis[3,3'-(1,4-butanediyl)-4,4',8,8',9,9'-hexaethyl-10,10'-dimethyl-2,2'-bidipyrinatopalladium(II)] (11): A suspension of 2· HClO_4 (85.0 mg, 0.11 mmol) and sodium methoxide (54 mg, 1.0 mmol) in methanol (5 mL) is stirred for 5 min. Zinc acetate hydrate (39 mg, 0.18 mmol) is then added at once, and the solution turns to dark green. After 30 min at ambient temperature the solvent is removed in vacuo, and the dark residue is extracted into pentane. The product is purified by alumina chromatography (basic alumina I) with dichloromethane/*n*-hexane (1:1), and the intense green main fraction is collected. Crystallization from dichloromethane/*n*-hexane (1:3) yields **11** as bronze-coloured plates. Yield 55.0 mg (84%). ^1H NMR (400 MHz, C_6D_6 , 25 °C): δ = 0.96 (t, 12 H, J = 7.4 Hz, $\text{CH}_3\text{CH}_2\text{pyr}$), 1.22 (t, 12 H, J = 7.4 Hz, $\text{CH}_3\text{CH}_2\text{pyr}$), 1.24 (t, 12 H, J = 7.3 Hz, $\text{CH}_3\text{CH}_2\text{pyr}$), 1.32–1.40 (m, 16 H, $\text{CH}_2\text{CH}_2\text{pyr}$ and $\text{CH}_2\text{CH}_2\text{pyr}$), 1.66 (s, 12 H, *term*- CH_3), 2.10–2.31 (m, 8 H, $\text{CH}_3\text{CH}_2\text{pyr}$), 2.51–2.61 (m, 16 H, $\text{CH}_3\text{CH}_2\text{pyr}$), 6.95 (s, 4 H, *meso*-H) ppm. $^{13}\text{C}\{^1\text{H}\}$ NMR (100 MHz, C_6D_6 , 25 °C): δ = 14.3, 14.4, 15.7, 17.9, 18.5, 23.0, 29.8, 30.1, 32.3, 120.3, 130.0, 137.8, 141.2, 143.5, 150.9, 159.7 ppm; the signals four two C(sp²) atoms are probably hidden underneath the solvent signal. HRMS (ESI) calcd. for $\text{C}_{72}\text{H}_{92}\text{N}_8\text{Zn}_2$: 1196.60275; obsd. 1196.60215, Δ = 0.60 mmu. UV/Vis (CH_2Cl_2): λ_{max} (ϵ , $\text{L mol}^{-1}\text{cm}^{-1}$) = 360 (52000), 475 (138000), 620 (48000) nm. $\text{C}_{72}\text{H}_{92}\text{N}_8\text{Zn}_2$ (1200.33): calcd. C 72.04, H 7.73, N 9.34; found C 71.72, H 7.39, N 9.05.

Crystallographic Data for 11: $\text{C}_{72}\text{H}_{92}\text{N}_8\text{Zn}_2$, green plates obtained by slow concentration of a CH_2Cl_2 /*n*-hexane solution, crystal size:

0.20 × 0.18 × 0.17 mm, triclinic, space group $P\bar{1}$, $a = 14.0038(16)$, $b = 20.206(2)$, $c = 24.556(3)$ Å, $\alpha = 72.719(2)$, $\beta = 84.446(2)$, $\gamma = 78.961(2)^\circ$, $V = 6505.9(13)$ Å³, $\rho_{\text{calcd.}} = 1.225$ g cm⁻³, $Z = 4$, $2\theta_{\text{max}} = 56.532^\circ$, Mo- K_α radiation, $\lambda = 0.71073$ Å, scan mode: ω -scans, $T = 153(2)$ K, 45469 measured, 22898 independent reflections, 17802 reflections observed for $I > 2\sigma(I)$, $\mu = 0.785$ mm⁻¹, solved by Patterson method, refined with full-matrix least-squares on F^2 [20], 1638 parameters and 107 restraints, H atoms refined with isotropic temperature factors. $R = 0.0607$, $wR = 0.1783$, residual electron density $\rho = 0.969/-0.641$ e Å⁻³.

3,3'-(1,4-Butanediyl)-4,4'-diethyl-8,8',9,9',10,10'-hexamethyl-2,2'-bidipyrinacopper(II) (12): A suspension of 1·2HClO₄ (50 mg, 0.07 mmol) in methanol (4 mL) was treated with a solution of copper acetate hydrate (20.0 mg, 0.10 mmol) in ammonia (1 mL of a conc. solution in water) at once. The colour immediately changed from dark green to brown. After 5 min the precipitated product was filtered off and washed with methanol. The solid was extracted with dichloromethane, again filtered, and the solution evaporated in vacuo to leave the title compound as a brown solid. Yield 25.0 mg (65%). M.p. 150 °C. EPR (293 K, CH₂Cl₂): $g_{\text{iso}} = 2.096$, $A_{\text{Cu}} = 82.1$ G. MS (FAB): 541 (M⁺). UV/Vis (CH₂Cl₂): λ_{max} (ϵ , L mol⁻¹ cm⁻¹) = 405 (57000), 495 (76000) nm. C₃₂H₃₈CuN₄ (542.217): calcd. C 70.88, H 7.06, N 10.33; found C 70.88, H 7.20, N 10.51.

Bis[3,3'-(1,4-butanediyl)-4,4'-diethyl-8,8',9,9',10,10'-hexamethyl-2,2'-bidipyrinacopper(II)] (13): A suspension of 1·2HClO₄ (50 mg, 0.07 mmol) and sodium acetate (40.0 mg, 0.48 mmol) in methanol (4 mL) was treated with a solution of copper acetate hydrate (20.0 mg, 0.10 mmol). The mixture turned brown, then dark green after 1 min of stirring. After 1 h at ambient temperature the solvent was removed in vacuo and the residue was extracted with pentane. Evaporation of the solvent yielded the title compound as a dark green powder. Yield 20.0 mg (54%). M.p. 108 °C (dec.). HRMS (ESI) calcd. for C₆₄H₇₆Cu₂N₈: 1082.47846; obsd. 1082.47874, $\Delta = 0.28$ mmu. UV/Vis (CH₂Cl₂): λ_{max} (ϵ , L mol⁻¹ cm⁻¹) = 410 (94000), 630 (29000) nm. C₆₄H₇₆Cu₂N₈ (1084.434): calcd. C 70.88, H 7.06, N 10.33; found C 70.55, H 6.87, N 10.01.

Crystallographic Data for 13: C₆₄H₇₆N₈Cu₂, red cubes obtained by slow concentration of a CH₂Cl₂/pentane solution, crystal size: 0.27 × 0.17 × 0.15 mm, orthorhombic, space group $Pbcn$, $a = 30.3691(19)$, $b = 25.1323(16)$, $c = 22.6084(14)$ Å, $V = 17255.8(19)$ Å³, $\rho_{\text{calcd.}} = 1.251$ g cm⁻³, $Z = 8$, $2\theta_{\text{max}} = 56.488^\circ$, Mo- K_α radiation, $\lambda = 0.71073$ Å, scan mode: ω -scans, $T = 173(2)$ K, 243067 measured, 15182 independent reflections, 12807 reflections observed for $I > 2\sigma(I)$, $\mu = 0.786$ mm⁻¹, solved by direct methods, refined with full-matrix least-squares on F^2 [20], 1061 parameters and 74 restraints, H atoms refined with isotropic temperature factors. $R = 0.1130$, $wR = 0.2517$, residual electron density $\rho = 1.111/-0.642$ e Å⁻³.

Acknowledgments

This work was funded by the Deutsche Forschungsgemeinschaft (DFG). The assistance of Dr. Dirk Leusser with the X-ray analysis of **11** is gratefully acknowledged.

- [1] See, e.g.: a) J. Subramanian, J.-H. Fuhrhop in *The Porphyrins* (Ed.: D. Dolphin), Academic Press, New York, **1978**, vol. 2, p. 255; b) R. Bonnett, D. G. Buckley, D. Hamzetaš, *J. Chem. Soc., Perkin Trans. 1* **1981**, 322; c) A. L. Balch, M. Mazzanti, B. C. Noll, M. M. Olmstead, *J. Am. Chem. Soc.* **1994**, 116,

- 9114; d) R. Koerner, M. M. Olmstead, A. Ozarowski, S. L. Phillips, P. M. Van Calcar, K. Winkler, A. L. Balch, *J. Am. Chem. Soc.* **1998**, 120, 1274; e) P. A. Lord, B. C. Noll, M. M. Olmstead, A. L. Balch, *J. Am. Chem. Soc.* **2001**, 123, 10554; f) L. Latos-Grażyński, J. Wojaczyński, R. Koerner, J. J. Johnson, A. L. Balch, *Inorg. Chem.* **2001**, 40, 4971; g) P. A. Lord, L. Latos-Grażyński, A. L. Balch, *Inorg. Chem.* **2002**, 41, 1011.
- [2] A. Wilks, *Antioxidants Redox Signaling* **2002**, 4, 603.
- [3] a) J.-H. Fuhrhop, A. Salek, J. Subramanian, C. Mengersen, S. Besecke, *Justus Liebig's Ann. Chem.* **1975**, 1131; b) P. K. W. Wasser, J.-H. Fuhrhop, *Ann. N.Y. Acad. Sci.* **1973**, 206, 533.
- [4] See e.g.: a) A. W. Johnson, I. T. Kay, R. Rodrigo, *J. Chem. Soc.* **1963**, 2336; A. W. Johnson, I. T. Kay, *J. Chem. Soc.* **1965**, 1620; P. Bamfield, R. Grigg, A. W. Johnson, R. W. Kenyon, *J. Chem. Soc., C* **1968**, 1259; A. Eschenmoser, *Pure Appl. Chem.* **1969**, 20, 1; J. Engel, H. H. Inhoffen, *Justus Liebig's Ann. Chem.* **1977**, 767; K. M. Barkigia, M. W. Renner, H. Xie, K. M. Smith, J. Fajer, *J. Am. Chem. Soc.* **1993**, 115, 7894; S. Neya, K. Nishinaga, K. Ohyama, N. Funasaki, *Tetrahedron Lett.* **1998**, 39, 5217; E. Vogel, B. Binsack, Y. Hellwig, C. Erben, A. Heger, J. Lex, Y.-D. Wu, *Angew. Chem.* **1997**, 109, 2725; *Angew. Chem. Int. Ed. Engl.* **1997**, 36, 2612; R. Paolesse in *The Porphyrin Handbook* (Eds.: K. M. Kadish, K. M. Smith, R. Guilard), Academic Press, San Diego/London, **2000**, vol. 2, p. 201; K. M. Smith in *The Porphyrin Handbook* (Eds.: K. M. Kadish, K. M. Smith, R. Guilard), Academic Press, San Diego/London, **2000**, vol. 1, p. 119.
- [5] a) H. Falk, *The Chemistry of Linear Oligopyrroles and Bile Pigments*, Springer, Vienna, **1989**; b) R. G. Khoury, M. O. Senge, J. E. Colchester, K. M. Smith, *J. Chem. Soc., Dalton Trans.* **1996**, 3937.
- [6] a) S. Yagi, T. Morinaga, T. Nomura, T. Takagishi, T. Mizutani, S. Kitagawa, H. Ogoshi, *J. Org. Chem.* **2001**, 66, 3848; b) S. Yagi, H. Sadachi, Y. Kashiwagi, T. Takagishi, T. Mizutani, S. Kitagawa, H. Ogoshi, *Chem. Lett.* **2000**, 1054; c) T. Mizutani, K. Wada, S. Kitagawa, *J. Org. Chem.* **2000**, 65, 6097; d) T. Mizutani, N. Sakai, S. Yagi, T. Takagishi, S. Kitagawa, H. Ogoshi, *J. Am. Chem. Soc.* **2000**, 122, 748; e) T. Mizutani, S. Yagi, A. Honmaru, T. Goldacker, S. Kitagawa, M. Furusyo, T. Takagishi, H. Ogoshi, *Supramol. Chem.* **1999**, 10, 297; f) S. Yagi, R. Yamada, T. Takagishi, N. Sakai, H. Takahashi, T. Mizutani, S. Kitagawa, H. Ogoshi, *Chem. Commun.* **1999**, 911; g) T. Mizutani, S. Yagi, T. Moninaga, T. Nomura, T. Takagishi, S. Kitagawa, H. Ogoshi, *J. Am. Chem. Soc.* **1999**, 121, 754; h) T. Mizutani, S. Yagi, A. Honmaru, S. Murakami, M. Furusyo, T. Takagishi, H. Ogoshi, *J. Org. Chem.* **1998**, 63, 8769; i) T. Mizutani, S. Yagi, A. Honmaru, H. Ogoshi, *J. Am. Chem. Soc.* **1996**, 118, 5318.
- [7] a) R. G. Khoury, L. Jaquinod, K. M. Smith, *Tetrahedron* **1998**, 54, 2339; b) Y. Zhang, A. Thompson, S. J. Rettig, D. Dolphin, *J. Am. Chem. Soc.* **1998**, 120, 13537; c) A. Thompson, S. J. Rettig, D. Dolphin, *Chem. Commun.* **1999**, 631; d) A. Thompson, D. Dolphin, *Org. Lett.* **2000**, 2, 1315; e) A. Thompson, D. Dolphin, *J. Org. Chem.* **2000**, 65, 7870.
- [8] a) G. Struckmeier, U. Thewalt, J.-H. Fuhrhop, *J. Am. Chem. Soc.* **1976**, 98, 278; b) W. S. Sheldrick, J. Engel, *J. Chem. Soc., Chem. Commun.* **1980**, 5.
- [9] a) T. E. Wood, A. C. Ross, N. D. Dalgleish, E. D. Power, A. Thompson, X. Chen, Y. Okamoto, *J. Org. Chem.* **2005**, 70, 9967; b) T. E. Wood, N. D. Dalgleish, E. D. Power, A. Thompson, X. Chen, Y. Okamoto, *J. Am. Chem. Soc.* **2005**, 127, 5740.
- [10] a) I. Spasojević, I. Batinić-Haberle, *Inorg. Chim. Acta* **2001**, 317, 230; b) I. Spasojević, I. Batinić-Haberle, R. D. Stevens, P. Hambright, A. N. Thorpe, J. Grodkowski, P. Neta, I. Fridovich, *Inorg. Chem.* **2001**, 40, 726.
- [11] a) H. S. Gill, I. Finger, I. Bozidarevic, F. Szydlo, M. J. Scott, *New J. Chem.* **2005**, 29, 68; b) L. Simkhovich, I. Goldberg, Z. Gross, *Org. Lett.* **2003**, 5, 1241; c) M. Bröring, D. Griebel, C. Hell, A. Pfister, *J. Porphyrins Phthalocyanines* **2001**, 5, 708; d) M. Bröring, *Synthesis* **2000**, 1291; e) H. Falk, H. Flödl, U. G.

- Wagner, *Monatsh. Chem.* **1988**, *119*, 739; f) D. Dolphin, R. L. N. Harris, J. L. Huppertz, A. W. Johnson, I. T. Kay, J. Leng, *J. Chem. Soc., C* **1966**, 98.
- [12] a) M. Bröring, E. Cónsul-Tejero, *J. Organomet. Chem.* **2005**, *690*, 5290; b) M. Bröring, C. D. Brandt, E. Cónsul-Tejero, *Z. Anorg. Allg. Chem.* **2005**, *631*, 1793; c) M. Bröring, C. D. Brandt, J. Bley-Esrich, J.-P. Gisselbrecht, *Eur. J. Inorg. Chem.* **2002**, 910; d) M. Bröring, C. D. Brandt, J. Lex, H.-U. Humpf, J. Bley-Esrich, J.-P. Gisselbrecht, *Eur. J. Inorg. Chem.* **2001**, 2549; e) M. Bröring, A. Pfister, K. Ilg, *Chem. Commun.* **2000**, 1407.
- [13] For the only exceptions see: a) K. T. Nguyen, S. P. Rath, L. Latos-Grażyński, M. M. Olmstead, A. L. Balch, *J. Am. Chem. Soc.* **2004**, *126*, 6210; b) A. L. Balch, L. Latos-Grażyński, B. C. Noll, M. M. Olmstead, L. Szterenber, N. Safari, *J. Am. Chem. Soc.* **1993**, *115*, 1422; c) A. L. Balch, L. Latos-Grażyński, B. C. Noll, M. M. Olmstead, N. Safari, *J. Am. Chem. Soc.* **1993**, *115*, 9056.
- [14] M. Bröring, C. Hell, C. D. Brandt, E. Cónsul Tejero, *J. Porphyrins Phthalocyanines* **2003**, *7*, 214.
- [15] V. Hegde, P. Madhukar, J. D. Madura, R. P. Thummel, *J. Am. Chem. Soc.* **1990**, *112*, 4549.
- [16] M. Bröring, S. Link, *Synthesis* **2002**, 67.
- [17] R. W. Saalfrank, *Angew. Chem.* **1977**, *89*, 184; *Angew. Chem. Int. Ed. Engl.* **1977**, *16*, 185.
- [18] A. Treibs, D. Dinelli, *Justus Liebigs Ann. Chem.* **1935**, 517, 152.
- [19] J. Tang, J. G. Verkade, *J. Org. Chem.* **1994**, *59*, 7793.
- [20] G. Sheldrick, *SHELXL-97, Program for Crystal Structure Refinement*, University of Göttingen, Germany, **1997**.

Received: October 19, 2006

Published Online: February 13, 2007